JA-243:022:88

Shallow-Water High-Frequency Bottom Scattering off Panama City, Florida

S. Stanic
K. B. Briggs
P. Fleischer
R. I. Ray
W. B. Sawyer

June 1988.

Naval Ocean Research and Development Activity
Stennis Space Center, Mississippi 39529-5004

Shallow-water high-frequency bottom scattering off Panama City, Florida

S. Stanic, K. B. Briggs, P. Fleischer, R. I. Ray, and W. B. Sawyer
Naval Ocean Research and Development Activity, NSTL, Mississippi 39529-5004

(Received 3 December 1987; accepted for publication 9 February 1988)

A series of bottom backscattering measurements was made in a flat, uniform, and isotropic area 19 miles south of Panama City, FL. Sidescan sonar, underwater television, stereo photography, high-resolution bathymetry, and sediment core analysis were used to locate and classify the experimental site. A sidescan sonar areal mosaic was contructed detailing the relationship between the experimental area and the surrounding topography. Bottom backscattering measurements were made as a function of frequency (20–180 kHz), grazing angle (5°–30°), azimuthal angle, and environmental conditions. Backscattering strengths were found to follow Lambert's law with little frequency dependence or measurable anisotropy. For this particular site, scattering strengths at 90 kHz were found to agree with predictions made using the Applied Physics Laboratory—University of Washington (APL—UW) model.

PACS numbers: 43.30.Gv, 43.30.Hw

INTRODUCTION

A large number of high-frequency bottom scattering measurements have been reported. However, the basic scattering mechanisms are still not completely understood. This understanding is essential for the development of improved environmental acoustic scattering models for high-frequency bottom reverberation. The Naval Ocean Research and Development Activity's (NORDA) high-frequency program focuses on the relationships between acoustic scattering and ocean bottom parameters.

Results of high-frequency bottom scattering measurements can be found in Urick,[1] Wong and Chesterman,[2] Bunchuk and Zhitkovskii,[3] McKinney and Anderson,[4] Roderick and Dullea,[5] Boehme *et al.*,[6] and Jackson *et al.*[7] Typically, bottom scattering has been correlated with four general bottom types: mud, sand, gravel, and rock. Measurements within each general bottom classification have shown little relation between scattering strength and particle or grain size.[8] Within each general sediment type, scattering strength can differ by 10–20 dB.

In general, bottom scattering has been found to be a function of $\sin^n \theta_g$, where θ_g is the grazing angle and n a number between 1 and 2. McKinney and Anderson[4] and Boehme *et al.*[6] found that for sand sediments, backscattering strength increases slightly with frequency. Bunchuk and Zhitkovskii[3] found little or no frequency dependence and discuss the possibility that sediment volume inhomogeneity rather than bottom surface roughness may be the dominant source of backscattering in shallow-water regions. However, Chotiros and Boehme[8] argue that, above 10 kHz, backscattering is primarily controlled by bottom roughness.

The approach of NORDA's high-frequency program has been to conduct a series of environmentally supported scattering measurements in areas that range from smooth, isotropic, and homogeneous to areas that are much more complex. It should then be possible to correlate acoustic scattering strengths and signal statistics with changes in bottom characteristics. This article details the environmental and acoustic backscattering measurements made during the initial series of experiments. The acoustic measurements were made using NORDA's acoustic instrumentation support towers.[9] Scattering strength measurements were made as a function of frequency (20–180 kHz), grazing angles (5°–30°), azimuthal angles, and pulse lengths (5 μs–10 ms) and were supported by sidescan sonar mapping, underwater television data, sediment core analysis, and stereo photography. Correlation and coherence estimates as a function of the above parameters will be reported in a second article. These measurements were conducted in 34 m of water in an area 19 miles south of Panama City, FL. This area was chosen because of its uniformity, relative lack of surface and buried shells, and for its smooth sandy surface. Measurements taken in this area will serve as the basis to which all other measurements taken in the program will be compared.

I. ENVIRONMENTAL MEASUREMENTS

In order to locate this special experimental area, a detailed environmental survey was conducted prior to the acoustic scattering experiments. Several large-scale areal surveys were used to identify potential acoustic measurement sites. The major systems used in these surveys are described in Stanic *et al.*[9] These include a Klein 100-kHz sidescan sonar system, a 3.5-kHz bottom profiler, and a 208-kHz high-resolution bathymetry system. These measurements were supported by underwater television, stereo photography, sediment core analysis, and diver observations.

Figure 1 details the sidescan survey tracks and dive locations used to locate the experimental area. Using precision Loran-C navigation, (0.01-μs time differences), a series of 150-m-wide sidescan sonar images were made of the experimental and surrounding area. The 150-m-wide swaths were then assembled into the mosaic shown in Fig. 2. A series of sounding lines made over the same area provided data for computer-generated sounding sheets from which a bathy-

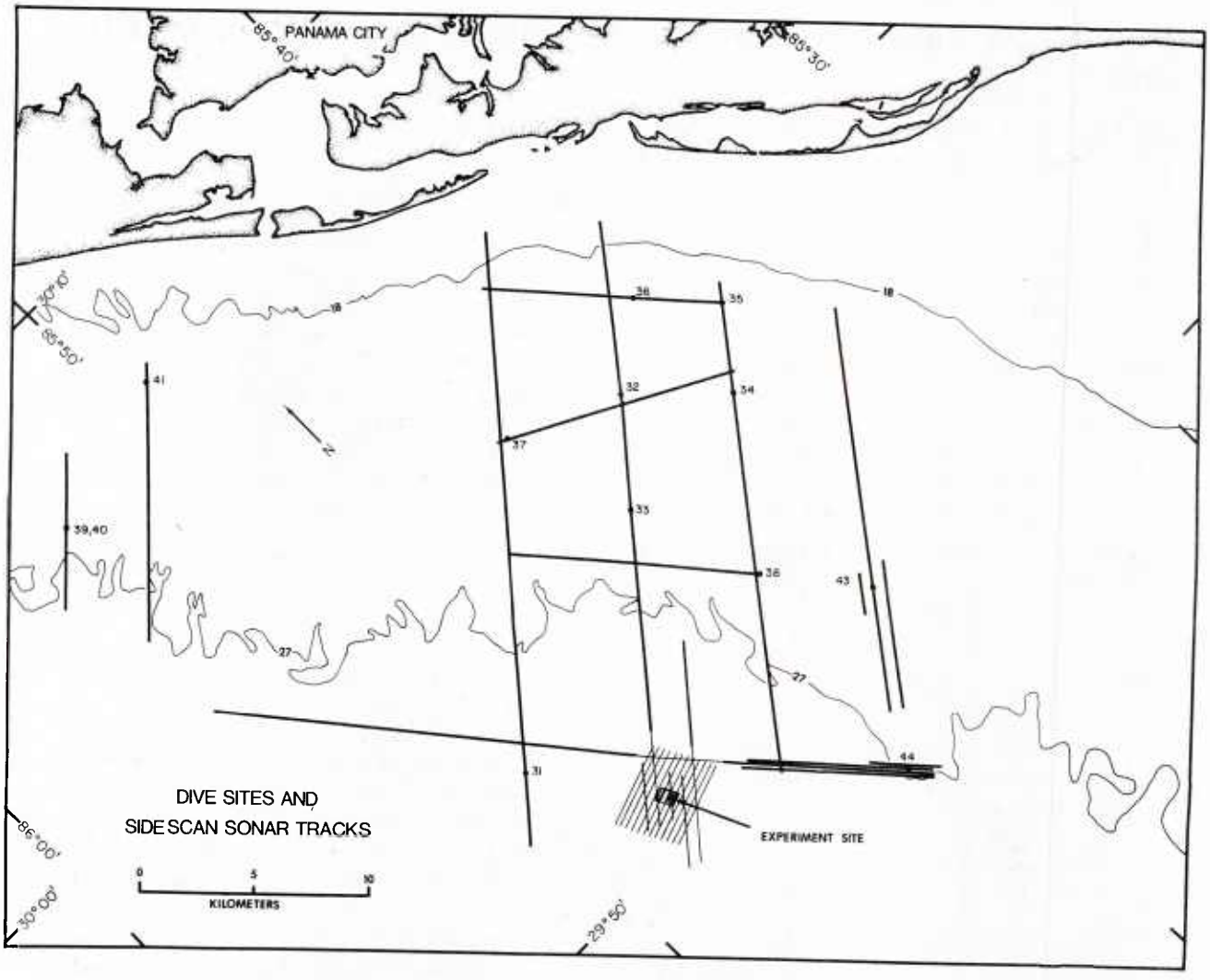

FIG. 1. Sidescan survey tracks and dive locations (numbered) used to locate the experiment site.

metric map of the area was constructed (Fig. 3). The bathymetric map displays the general morphology of the area. It was used to evaluate the bottom slope and to quantify any large-scale roughness. The actual experimental site, about 1 km^2, was imaged at greater resolution by mapping with sidescan sonar at a 50-m range and with a high-density bathymetric survey. The sounding density was sufficient for the bottom relief to be mapped with 0.1-m isobaths (Fig. 4) so that minor variations and irregularities in bottom character and bathymetry could be detected.

The areal setting of the experiment site (Fig. 2) is typical of the inner- and midshelf regions of the northeastern Gulf of Mexico, and is similar to sandy inner shelves in general. The seafloor exhibits a subdued, north–south trending ridge morphology, with wavelengths of about 200–1000 m and amplitudes of 1–3 m. The ridges are slightly asymmetric, the steep sides facing east. The reflectivity variations displayed on the mosaic are not due directly to relief (roughness > 10 cm), but are caused by variation in sediment character and microrelief (10 cm $>$ roughness $>$ 1.5 cm). The light areas (low reflectivity) are typically fine, featureless sand with little or no microrelief; the bands of reflective bottom are composed of coarser, somewhat shelly sand, sometimes shaped into ripple fields. These bands do not correspond to the ridge troughs, as often observed, but instead occupy the steep flank of the ridge, and terminate abruptly in the trough. Even though the area shows considerable, if somewhat regular variability in bottom character, the 1-km^2 experiment site, from a large-scale viewpoint, is essentially flat and of uniform sediment character. These high-resolution surveys of the experimental site allow extrapolation of detailed but localized photogrammetric and sediment property measurements to the entire site.

Sediment core analysis and surface roughness measurements were used to classify the small-scale features of the experimental site. Sample locations were chosen using the areal mosaic and estimates of the acoustic patch size and locations.

Sediment samples were collected by divers using 6.1-cm (ID) cylindrical cores. Collection, measurement, and handling procedures were designed to minimize sampling disturbance and to maintain an intact sediment–water interface

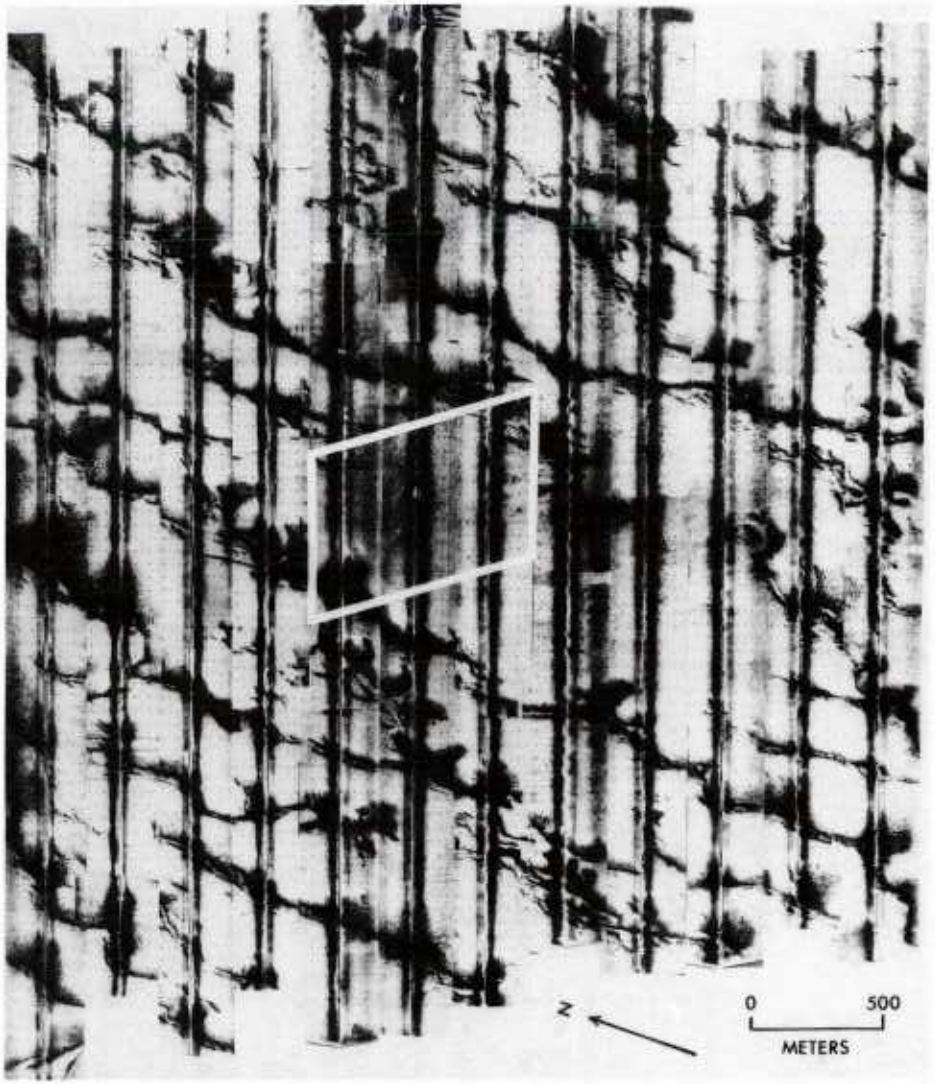

FIG. 2. Sidescan sonar mosaic of experiment site and surrounding area. Box indicates area of detailed surveys and acoustic measurements.

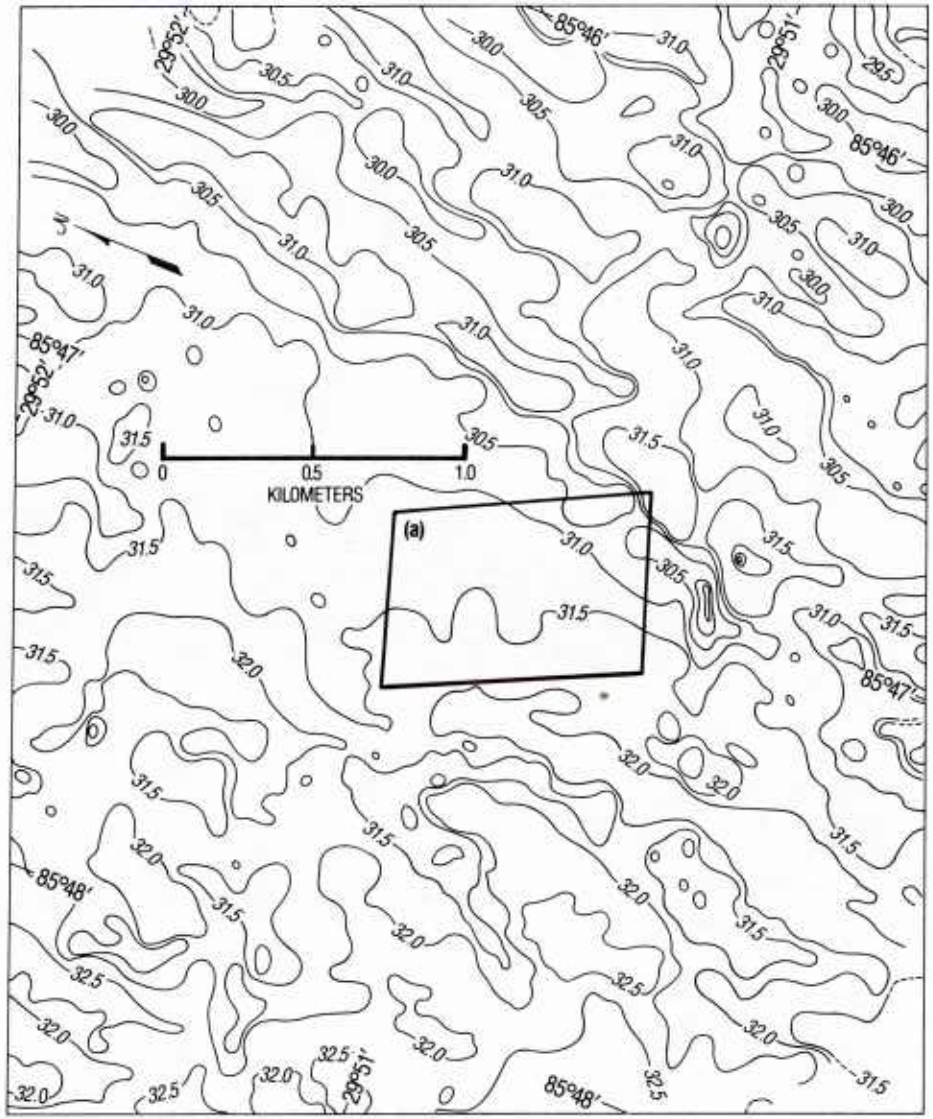

FIG. 3. Bathymetric map of experiment site (a) and surrounding area. Isobaths in meters.

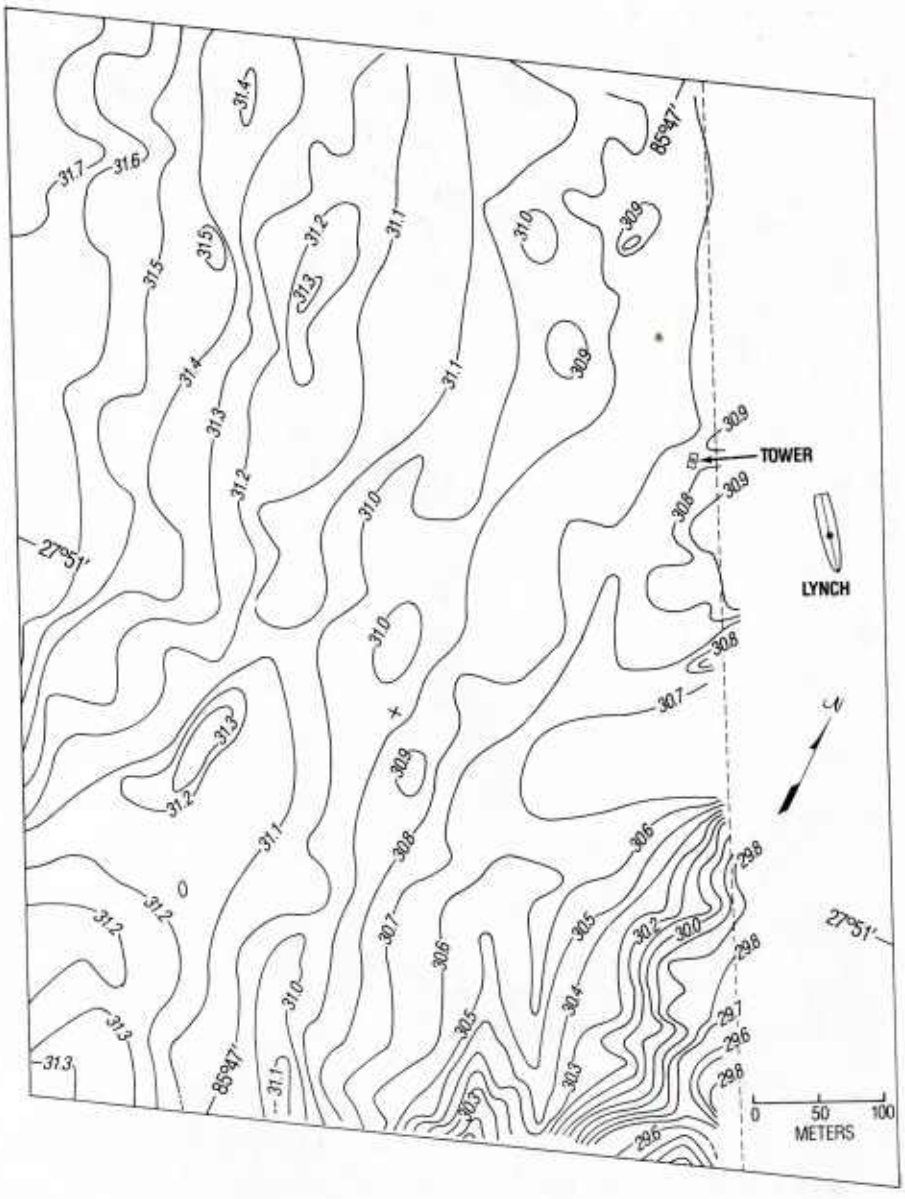

FIG. 4. High-resolution map of experiment site (a). This map and the one shown in Fig. 3 were constructed from two separate bathymetric surveys; Hence, there is some variation of isobaths within area (a). Isobaths in meters.

within the core samples. Sediment compressional wave velocity and attenuation were measured aboard ship, after the sediments had equilibrated with the ship's laboratory temperature (usually 24 h after collection). Sediment compressional wave velocity and attenuation were measured at 1-cm intervals in 15 cores using a pulse technique.[9]

Time delay measurements of a 400-kHz cw pulse were made through the sediments and a distilled water reference using an Underwater Systems, Inc. (model USI-103) transducer–receiver head. Differences in time delay between distilled water and sediment samples were used to calculate sediment compressional wave velocity. Compressional wave velocity was expressed as the ratio of measured sediment velocity to measured velocity for the overlying water at the same temperature, salinity, and depth.[10] This ratio is independent of sediment temperature, salinity, and depth and can be used as an input for predictive acoustic models. Attenuation measurements were calculated as 20 log of the ratio of received voltage through distilled water to received voltage through sediment.[11] Values of compressional wave attenuation were extrapolated to a 1-m path length and expressed as dB/m.

Upon completion of acoustic measurements on the sediment cores, samples were extruded and sectioned at 2-cm intervals to determine sediment porosity, density, and grain size distribution. Porosity was determined from weight loss of sediment dried at 105 °C for 24 h and from average grain density measurements of dried sediment made with an air comparison pycnometer. Values of porosity were not corrected for pore water salinity. Salt-free porosity may be obtained by multiplying values by 1.012. Sediment density was calculated from values of porosity and average grain density and expressed as the ratio of sediment density to overlying water density. Sediment grain size was determined from disaggregated samples by dry sieving for sand-sized particles at every phi interval and by pipette for silt- and clay-sized particles. Grain size statistics were determined from the graphic formulas of Folk and Ward.[12]

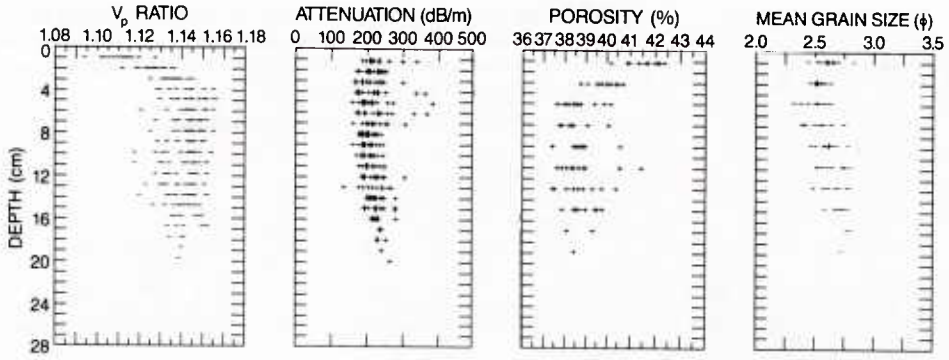

FIG. 5. Vertical distributions of sediment compressional wave velocity, attenuation, porosity, and mean grain size.

The vertical distribution of sediment geoacoustic properties for the 15 cores collected at the experiment site are displayed in Fig. 5. Values of sediment compressional wave velocity (V_p ratio), attenuation, porosity, and mean grain size (phi) exhibited relatively low variability in the top 25 cm of surficial sediment when compared with other shallow-water areas.[13]

Compressional wave velocity ratio values average 1.133 with a coefficient of variation of 0.87%. Sediment compressional wave velocity at *in situ* conditions (24 °C; 36 ppt; 34 m) ranges from 1677–1763 m/s (mean: 1737 m/s). The only discernible trend in sediment sound velocity is a slight increase down to 4-cm depth, then a constant velocity below 4-cm sediment depth.

Sediment compressional wave attenuation values at 400 kHz average 234 dB/m with a coefficient of variation of 15.60%. Compressional wave attenuation at the experiment site ranged from 168–393 dB/m. Assuming a linear relationship between attenuation and frequency, attenuation at 20 kHz was calculated to be 11.7 dB/m.[11] Variability of the attenuation values at various depths in the sediment is thought to be caused by the presence of mollusk shell fragments. Scattering of the 400-kHz acoustic signal by gravel-sized (>1 mm) shell fragments at this experiment site is minimal compared to other shallow-water sites.[14,15]

Values of sediment porosity average 39.0% with a coefficient of variation of 3.72%. Sediment porosity at the experiment site ranges from 34.6%–42.5%. There is a slight decrease in porosity with depth in the sediment. Sediment density calculated[9] from porosity and average grain density (2.65 g/cm^3) averaged 2.016 g/cm^3. Average sediment density ratio (sediment density divided by seawater density) is calculated to be 1.966.

Values of sediment mean grain size average 2.59 phi (0.166 mm) with a coefficient of variation of 6.16% in the 15 cores from the experiment site analyzed for grain size distribution. The sediments are characterized by moderately sorted to poorly sorted, fine-skewed to coarse-skewed, and leptokurtic to very leptokurtic fine sands. There is little variation in mean grain size with depth in the sediment, although coarse-skewed distributions occur at 5 and 20 cm due to the presence of some gravel-sized shell fragments.

Bottom roughness was determined from stereo photographs made with a 35-mm stereo underwater camera (Photosea model 2000 M), with a 100-W·s underwater strobe (Photosea model 1000 S) mounted in a molded fiberglass module. The camera was mounted in a rigid PVC pipe frame to allow the diver to maintain a constant focal distance (91 cm) and orientation with respect to the bottom. Two Nikon UW-NIKKOR 28-mm lenses, separated by 61 mm, resulted in a 55-$\times$72-cm image overlap. A glass "reseau" plate between the lenses and the film superimposed a precise arrangement of fiducial marks on the images. These reticle marks were used in the subsequent photogrammetric analysis.

Prior to beginning a photographic transect, the orientation was determined using a diver's compass and a 15-m-long tape measure. A photographic transect was made that coincided with the 270° azimuthal direction of the acoustic measurements. Because of the uniformity of the area, only two photographic dives were needed. Station 69 was located 20 m west of the acoustic tower and station 75 was located 50 m west of the tower.

The stereo photographs were processed as continuous rolls and examined for clarity and exhibition of representative bottom features in the experiment area. From the total of 55 bottom stereo photographic pairs made on two separate dives, 25 were chosen for photogrammetric analysis. Each stereo pair was analyzed with a Seagle 90 subsea photogrammetric stereocomparator and a Zenith ZDS 248 microcomputer. Calibration of the camera lenses at the focal distance used in the experiment was done by the developer of the photogrammetric software, Benima (Hasselblad) AB, Göteborg, Sweden. Spatial accuracy of better than 1 mm can be expected from this analysis.[9]

Relative sediment height was determined for 128 equally spaced (0.42 cm) points along six digitized transects, or cross-sectional lines in each stereo pair. Three cross-sectional lines (53.34 cm long) were oriented parallel to the tape measure on the sea bottom (270°) and three lines were oriented perpendicular to the tape measure (0°). Optical distortion was apparent in 74 of the 150 cross-sectional lines and these data were eliminated from further analysis.

Bottom roughness characterized by rms height and power spectra were estimated from 76 sets of digitized cross-sectional lines. The power spectral density function was estimated for each set of 128 points using procedures developed by D.B. Percival of the Applied Physics Laboratory, University of Washington.[16] The power spectral density function was averaged for each photographic location (stations 69 and 75) and orientation (270° and 0°).

Underwater color video data and stereo photographs

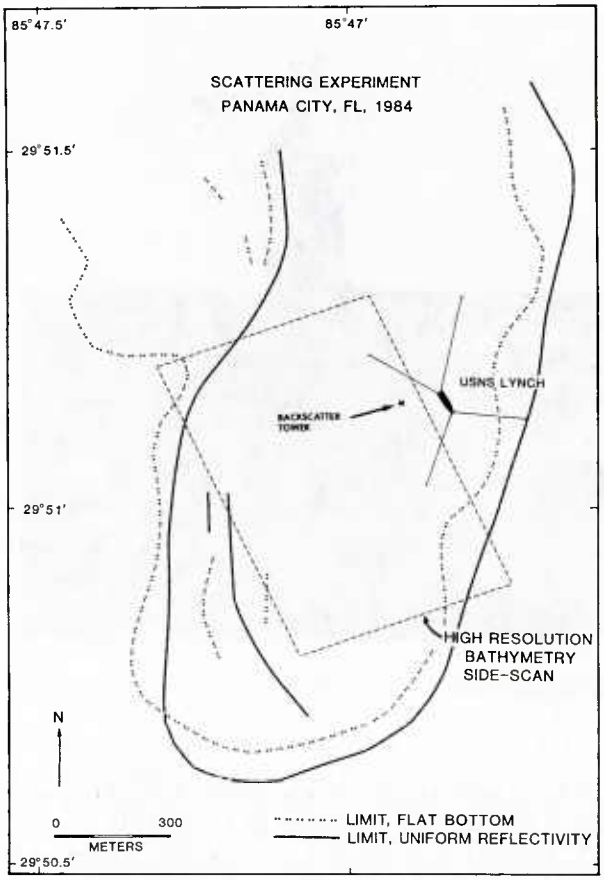

FIG. 11. Experiment setting with definition of experiment site by bottom uniformity and relief constraints.

m along the maximum response axis, TL is the transmission loss in dB, and A is the effective insonified bottom area in m^2.

Since the beam pattern of the parametric sources were circularly symmetric, the effective insonified areas were the areas of the projection of the circular area at the 3-dB down points of the main beam where it intersects the bottom. This assumes that the grazing angle is constant over the instantaneous area. This is acceptable because the linear sound-speed profile did not produce any focusing or shadowing in the measurement areas. In cases where the area was pulse-length limited, the area was defined as:

$$A = r\beta[(c_b\tau/2)\sec\theta_g],$$

where r is the horizontal range, c_b is the sound speed just above the bottom, τ is the pulse length, β is the effective beam width of the projector and receiving hydrophone, and θ_g is the grazing angle.

IV. BOTTOM BACKSCATTERING RESULTS

A. Grazing angle dependence

Acoustic backscattering strength measurements were made as a function of frequency, grazing angle, pulse length, and azimuthal angle. The scattering strength estimates were made using data from the hydrophone positioned at the center of the array. Figure 12 shows scattering strength esti-

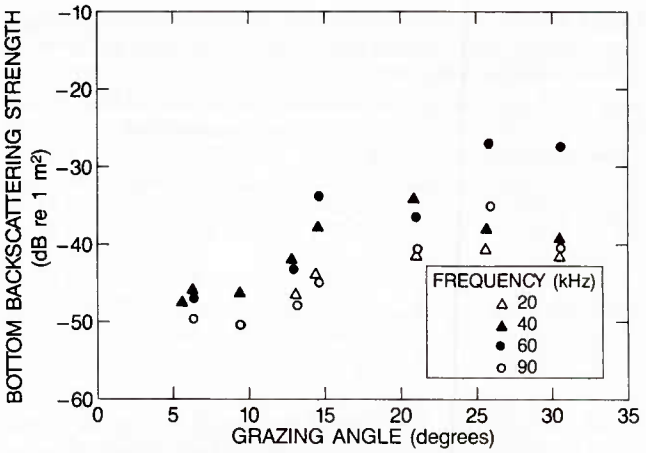

FIG. 12. Backscattering strength versus grazing angle.

mates versus grazing angle at frequencies of 20, 40, 60, and 90 kHz. Variations in scattering strength with frequency cannot be related to grain size. The values at 20 kHz for this site are 2–4 dB lower than those measured by Jackson *et al.*[7] at a site in the North Sea. The average grain size at the North Sea site was 0.199 mm. Measurements taken by Jackson *et al.*[7] at a Puget Sound site are 1–3 dB lower at 20 kHz but are 2–5 dB higher at 40 kHz. The average grain size in this area was 0.035 mm. Low-grazing angle scattering measurements taken by Boehme *et al.*[6] in San Diego are about 3 dB higher at 60 kHz. The average grain size at the San Diego site was 0.09 mm.

Figure 13 gives high-frequency scattering strength estimates (110, 150, and 180 kHz) versus grazing angle. These values tend to show the same general functional characteristic as the lower frequency scattering strength estimates. No correlation between scattering strength, frequency, and grain size was evident at these higher frequencies.

Figures 14–16 give scattering strength estimates as a function of both grazing angle and azimuthal angle. As expected, these results show little azimuthal dependence.

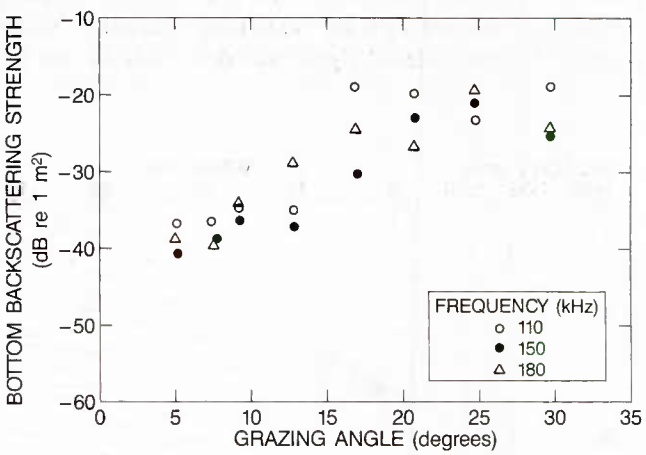

FIG. 13. Backscattering strength versus grazing angle.

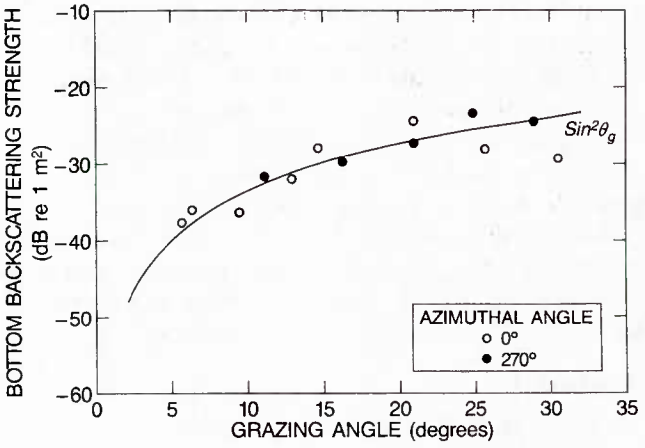

FIG. 14. Azimuthal dependence of bottom backscatter at 40 kHz.

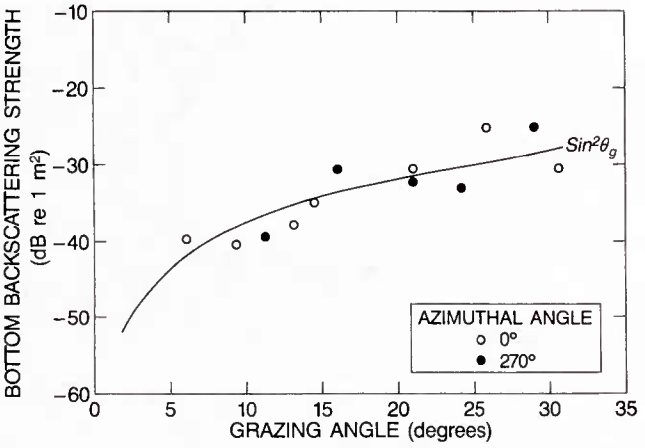

FIG. 16. Azimuthal dependence of bottom backscatter at 150 kHz.

These results further support the measurements detailing the isotropic and homogeneous nature of the bottom.

Figure 17 is a comparison of measured rms roughness with scattering strength calculations for the San Diego,[6] Puget Sound,[7] Charleston,[18] and Panama City data. This shows a lack of scattering strength dependence on rms bottom roughness. Scattering strengths at low grazing angles should be sensitive to change in rms roughness. However, rms roughness is a simple descriptor of a very complex surface. It provides no direct relationship between bottom roughness slope and the spectral characteristics of acoustic signals and bottom roughness contours. More emphasis should be directed towards describing the bottom in terms of its spectral characteristics.

The scattering strength measurements were made using 5- and 10-ms-long cw pulses. There was no apparent dependence of the scattering strength estimates on pulse length.

Errors in scattering strength estimates occur from the calibration of the hydrophones and parametric sources. It is estimated that these are on the order of 1–2 dB. During the course of the experiment, the water column environment was stable with sea states less than 1 ft. Signal fluctuations, which could further introduce error, were primarily due to marine life that migrated to the tower.

B. Frequency dependence

Bottom backscattering can also be expressed as[1]

$$\mathrm{BS} = 10 \log \mu + 20 \log \sin \theta_g \quad \text{(Lambert's law)},$$

where θ_g is the grazing angle and $10 \log \mu$ is the backscattering strength at normal incidence.

A $\sin^2\theta_g$ curve was fitted to each set of backscattering data and a value of $10 \log \mu$ was estimated. Examples are shown in Figs. 14–16. Scattering strength at the other frequencies also tended to have a $\sin^2\theta_g$ dependence. Figure 18 is a plot of $10 \log \mu$ as a function of transmitted frequency. The error bars are the standard deviations of the data. For this sandy smooth bottom, the scattering strengths increased by about 1.5 dB/oct. Jackson's Puget Sound data[7] showed a slope of 1.4 dB/oct, while the North Sea data had a slope of -0.2 dB/oct. Data for the sandy region at San Diego[6] showed a frequency dependence of 3 dB/oct.

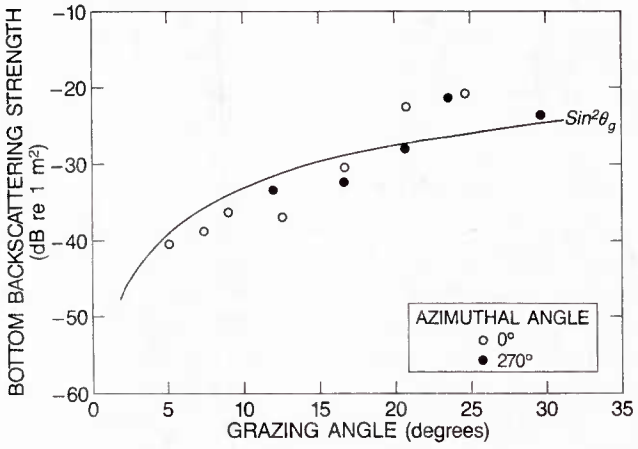

FIG. 15. Azimuthal dependence of bottom backscatter at 90 kHz.

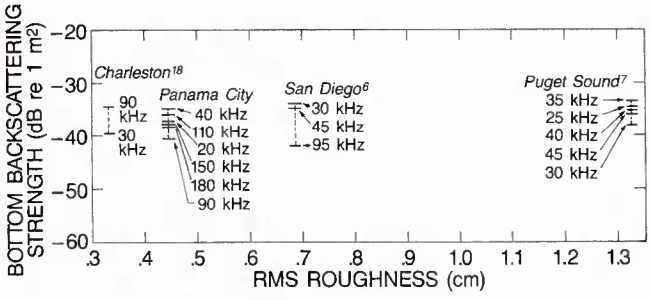

FIG. 17. Comparison of bottom backscattering strengths versus rms roughness for an 8° grazing angle.

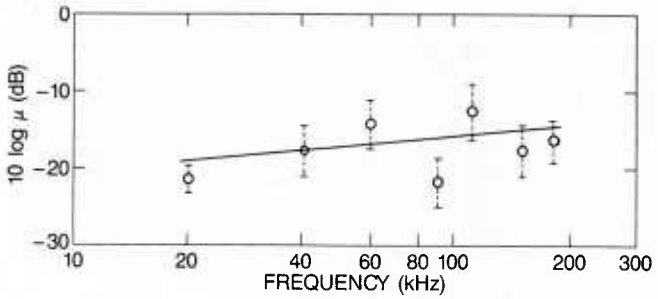

FIG. 18. Frequency dependence.

V. MODEL COMPARISION

A semiempirical model developed by Jackson *et al.*[19,20] was used to compare predictions of high-frequency bottom backscattering derived from the environmental data to the experimental data. The model is a simplification of the composite roughness model that generates bottom backscatter strength at various acoustic frequencies over a broad range of grazing angles. Backscattering predictions using this model require four environmental inputs: sediment compressional velocity ratio, sediment density ratio, sediment volume scattering parameter, and bottom roughness parameter. For this homogeneous experimental site, mean values of the geoacoustic parameters were used for the model inputs. For this sandy bottom, the sediment volume scattering parameter was assigned a value of 0.004.[19,20]

Jackson's model requires that the rms roughness values given in Table I be extrapolated to a 100-cm path length. The model also assumes a power spectral density slope of -2.25.

Scattering strength predictions for the two orthogonal azimuthal angles at station 69 are shown in Fig. 19. These predictions were made for an acoustic frequency of 90 kHz using a velocity ratio of 1.133 and a density ratio of 1.966. Figure 19 also compares these predicted values with the measured data. Even though the slope of the measured power spectral density function was not -2.25, it apparently is close enough to our experimental value of -1.92 to allow the model to produce a reasonable fit to the data points. The corresponding model inputs produce the same results for station 75. Differences in predicted backscattering strengths between the two orientations are on the order of 2 dB.

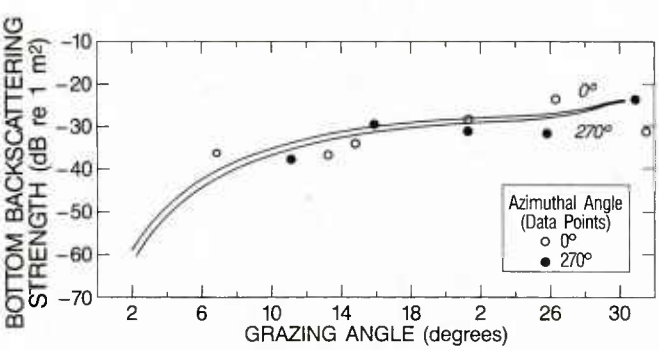

FIG. 19. Comparison of backscattering strength predictions with experimental results for station 69.

Additional data are now needed for an area where the surface roughness is dominated by anisotropic sand waves or ripples. Data are also needed for a sandy area where there are a significant number of sediment volume scatterers. The model should be updated so it can use measured volume scattering coefficients. In addition, the model would benefit from modifications to accept the true slope of the roughness power spectral density since the assumed power spectral slope value of -2.25 is for a very special case.

VI. SUMMARY

The geoacoustic and, to a large extent, bottom roughness data, demonstrate the homogeneous character of the seafloor at the 1-km^2 experiment site. The seafloor at the experiment site was essentially a featureless, isotropic region of hard-packed fine sand. Although statistical differences exist between the slopes of the roughness power spectra at different locations, there are no significant differences in rms roughness between different locations, and roughness is isotropic in terms of power spectral density and rms roughness. A comparison of coefficients of variation for sediment porosity, grain size, compressional wave velocity, and attenuation with those of other shallow-water environments demonstrates that this experiment site exhibits less variation in geoacoustic properties than most shallow-water sites.[13]

Bottom backscattering estimates showed a frequency dependence of 1.5 dB/oct and tended to follow Lambert's law over the range of frequencies, grazing angles, and pulse lengths used. Scattering strengths also showed no dependence on measured rms roughness. No anisotropy was observed at grazing angles between 5° and 30° which is consistent with the uniformity of the experimental area.

Even though the slope of the measured power spectral density function was not the assumed value, predictions made with Jackson's composite roughness model produced a reasonable fit to the experimental points. The selection of a low value for the sediment volume scattering parameter was valid because this area did not have an abundance of sediment volume scatterers.

NORDA has conducted a second experiment off the east coast of Florida that was characterized by a thick layer of large shell hash. These scattering strength results will be reported shortly. A third experiment is planned in an area south of Panama City, FL, where the bottom is characterized primarily by sand waves or ripples.

ACKNOWLEDGMENTS

The authors particularly thank L. Carlton and W. Clay of the Naval Underwater Systems Center, New London, CT, for development of the parametric acoustic sources. We also thank R. Love, R.W. Farwell, and D.R. Jackson for their helpful comments. Thanks are due to the Naval Coastal Systems Center, Panama City, FL, for cooperation with logistics and support for staging and testing. This work was supported by Office of Naval Research, Program element 61153N, through the NORDA Defense Research Sciences Program, NORDA contribution No. 243:022:88.

[1]R. J. Urick, *Principles of Underwater Sound* (McGraw-Hill, New York, 1975).
[2]H.-K. Wong and W. D. Chesterman, "Bottom backscattering near grazing incidence in shallow water," J. Acoust. Soc. Am. **44**, 1713–1718 (1968).
[3]A. V. Bunchuk and Yu. Yu. Zhitkovskii, "Sound scattering by the ocean bottom in shallow-water regions (review)," Sov. Phys. Acoust. **26**, 363–370 (1980).
[4]C. M. McKinney and C. D. Anderson, "Measurements of backscattering of sound from the ocean bottom," J. Acoust. Soc. Am. **36**, 158–163 (1964).
[5]W. I. Roderick and R. K. Dullea, "High resolution bottom backscattering measurements," Naval Underwater Systems Center, NUSC Tech. Doc. 7181 (June 1984).
[6]H. Boehme, N. P. Chotiros, L. D. Rolleigh, S. P. Pitt, A. L. Garcia, T. G. Goldsberry, and R. A. Lamb, "Acoustic backscattering at low grazing angles from the ocean bottom. Part I. Bottom backscattering strength," J. Acoust. Soc. Am. **77**, 962–979 (1985).
[7]D. J. Jackson, A. M. Baird, J. J. Crisp, and P. A. G. Thomson, "High-frequency bottom backscatter measurements in shallow water," J. Acoust. Soc. Am. **80**, 1188–1199 (1986).
[8]N. P. Chotiros and H. Boehme, "High-frequency environmental acoustics bottom backscattering analysis," Applied Reseach Laboratories, University of Texas at Austin, ARL-TR-86-27 (October 1986).
[9]S. Stanic, P. Fleischer, K. B. Briggs, M. P. Richardson, and B. Eckstein, "High-frequency acoustic bottom scattering experiments, Part I. Instrumentation and methods," Naval Ocean Research and Development Activity, Rep. No. 178 (January 1987).
[10]E. L. Hamilton, "Sound velocity and related properties of marine sediments, North Pacific," J. Geophys. Res. **75**, 4423–4446 (1970).
[11]E. L. Hamilton, "Compressional wave attenuation in marine sediments," Geophysics **37**, 620–645 (1972).
[12]R. L. Folk and W. C. Ward, " Brazos River bar, a study in the significance of grain size parameters," J. Sediment. Petrol. **27**, 3–26 (1957).
[13]M. D. Richardson, "Spatial variability of surficial shallow water geoacoustic properties," in *Ocean Seismo-Acoustics*, edited by T. Akal and J. M. Berkson (Plenum, New York, 1986), pp. 527–536.
[14]M. D. Richardson, K. B. Briggs, R. I. Ray, and W. H. Jahn, "Environmental support for high-frequency acoustic experiments conducted at the Quinault Range off the Washington coast, 28 April–1 May 1983," Naval Ocean Research and Development Activity, Rep. 132 (NORDA, NSTL, MS, 1986).
[15]K. B. Briggs, P. Fleischer, R. I. Ray, W. B. Sawyer, D. K. Young, M. D. Richardson, and S. Stanic, "Environmental support for a high-frequency acoustic bottom backscatter experiment off Charleston, South Carolina, 17–28 June 1983," Naval Ocean Research and Development Activity Rep. 130, (NORDA, NSTL, MS, 1986).
[16]D. B. Percival, Applied Physics Laboratory, University of Washington (1985) (private communication).
[17]P. Bloomfield, *Fourier Analysis of Time Series: An Introduction* (Wiley, New York, 1976).
[18]H. Boehme, N. P. Chotiros, and D. J. Churay, "High-frequency environmental acoustics bottom backscattering results," Applied Research Laboratories, University of Texas at Austin, ARL-TR-85-30 (Oct. 1985).
[19]D. R. Jackson, D. P. Winebrenner, and A. Ishimaru, "Application of the composite roughness model to high-frequency bottom backscattering," J. Acoust. Soc. Am. **79**, 1410–1422 (1986).
[20]D. R. Jackson, "Third report on TTCP bottom scattering measurements: model development," APL-UW Rep. 8708 (APL-University of Washington, Seattle, WA, 1987).